ACS Synthetic Biology
Cite This: ACS Synth. Biol. 2019, 8, 1241−1248
Letter
pubs.acs.org/synthbio

Driving the Scalability of DNA-Based Information Storage Systems

Kyle J. Tomek,[†,⊥] Kevin Volkel,[‡,⊥] Alexander Simpson,[‡] Austin G. Hass,[†,§] Elaine W. Indermaur,[†] James M. Tuck,[*,‡] and Albert J. Keung[*,†]

[†]Department of Chemical and Biomolecular Engineering, North Carolina State University, Raleigh, North Carolina 27695, United States

[‡]Department of Electrical and Computer Engineering, North Carolina State University, Raleigh, North Carolina 27695, United States

[§]Department of Structural and Molecular Biochemistry, North Carolina State University, Raleigh, North Carolina 27695, United States

Supporting Information

ABSTRACT: The extreme density of DNA presents a compelling advantage over current storage media; however, to reach practical capacities, new systems for organizing and accessing information are needed. Here, we use chemical handles to selectively extract unique files from a complex database of DNA mimicking 5 TB of data and design and implement a nested file address system that increases the theoretical maximum capacity of DNA storage systems by five orders of magnitude. These advancements enable the development and future scaling of DNA-based data storage systems with modern capacities and file access capabilities.

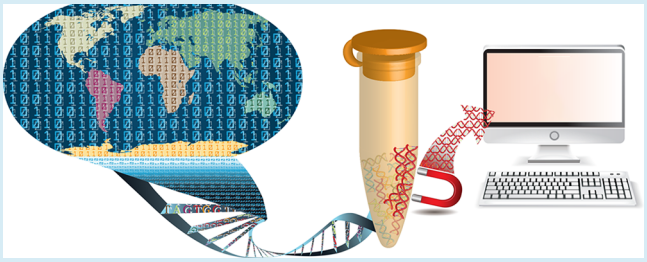

KEYWORDS: *synthetic biology, DNA storage, information storage, nested architecture, file access, DNA sequencing*

DNA is an excellent candidate for archival data storage as it offers high raw information density as well as durability and energy efficiency.[1−4] Motivated by these compelling properties, pioneering work has tackled many important features needed for a DNA storage system. For example, encoding and decoding algorithms have been developed to be tolerant to errors while also being highly efficient in terms of density and computational intensity.[5−13] Strategies such as nested polymerase chain reaction (PCR) architectures have also been proposed to increase the number of file addresses in storage systems.[14] In addition, molecular manipulations have been developed to access files through PCR amplification,[8,9,11,15,16] encrypt and rewrite information using PCR and Sanger sequencing,[8,17] and implement DNA-based computations or search functionalities through extraction of specific DNA strands using biotin-functionalized DNA oligomers.[18,19] Further accelerating the field, a recent implementation of a 200 MB DNA storage system demonstrated that current DNA synthesis technologies are already capable of reasonable modern storage capacities.[15]

Given these rapid advancements in DNA storage, it is timely to anticipate the challenges that will arise as systems continue to scale in capacity and density. Broadly encompassing these challenges is the fact that as systems continue to scale, DNA databases will become ever more diverse, crowded, and physically disordered, thus posing inherent barriers to data organization and retrieval. This analysis can be broken down further into specific issues. For example, existing systems have few enough strands to be completely read by modern DNA sequencing technologies; in contrast, future high-capacity systems will not be able to be sequenced in their entirety (Figure 1, Supplementary Figure 1), nor will entire databases be able to be decoded and stored using low latency systems with much smaller capacities that are higher in storage hierarchies (i.e., semiconductor-based systems). In addition, high-capacity DNA storage systems will also require a large number of available file addresses (i.e., PCR primer sequences[5,8−12,15,16]) to organize the data. However, due to increasing probabilities for potential off-target molecular interactions as systems scale in capacity, addresses must be sufficiently different from each other in sequence and are, therefore, finite in number and limit total system capacities (Figure 1, Supplementary Figure 1).

Our goal was to develop a robust platform with an easy to adopt implementation that could address these capacity limitations. Here, we leverage, innovate, and integrate prior[14,18,19] and new robust biomolecular tools and encoding strategies to implement a platform capable of scaling storage system capacities. In particular, we present a system for nondestructively accessing specific data from high-capacity DNA-based databases in conjunction with a nested file address system that can handle the organization of exascale databases. We refer to this overall storage system, which uses DNA

Received: March 4, 2019
Published: May 22, 2019

DOI: 10.1021/acssynbio.9b00100
ACS Synth. Biol. 2019, 8, 1241−1248

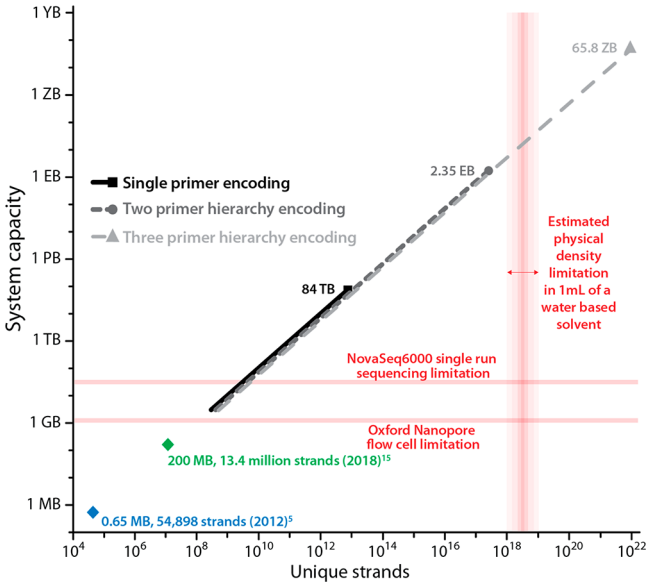

Figure 1. Theoretical analysis of readable files sizes, total system capacity limits, and improvements through physical data extraction and nested encoding. Limited readable files sizes: Current sequencing platforms can only sequence a fraction (~20−30 GB) of the theoretical maximum capacity of current systems (84 TB) assuming a sequencing depth of 10. Capacity limits: The linear plots of system capacities are based on current best estimates of 28 000 usable primers[15] and an average file size stored per unique address of 3 GB. As the total number of unique strands within a database increases, so does the total system capacity, limited ultimately by the number of primers available. Thus, the availability of noninteracting primers limits the theoretical maximum capacity of storage systems. The system capacity limit for current one-primer encodings using 28 000 primers (all 27 999 files sharing 1 antisense primer) storing 3-GB files is 84 TB (total capacity = total file addresses × file size); this corresponds to 7.88×10^{12} unique 200 bp long strands. In contrast, using the same distinct primers in double or triple nested architectures increases the number of possible addresses exponentially (total file addresses = $27\,999^{\text{N number of nests}}$). As a result, the total capacities also increase to 2.35 EB (2.52×10^{17} unique strands) and 65.8 ZB (8.98×10^{21} unique strands), respectively. The limits of commonly used next generation sequencing platforms are included for reference: Oxford nanopore flow cells can sequence 1.5×10^{11} bases or roughly 1.27 GB per flow cell using our encoding scheme and average sequencing depth of 10. Illumina's Novaseq6000 platform can sequence 2×10^{10} of our 200 bp strands per run or roughly 28.9 GB. The aqueous solubility of DNA is roughly between 10^{18} and 10^{19} per milliliter, depending on ionic concentrations.

Enrichment and Nested SEparation, as DENSE data storage. This system, through the integrated use of magnetic bead purifications and nested PCR primers, directly addresses the challenges arising from the molecularly crowded nature of high-capacity DNA storage systems while functioning within a single physical pool of DNA. Therefore, it not only harnesses the raw capacity and density advantages of DNA but also drives the practical scalability of high-capacity data storage systems.

The current state-of-the-art file access method uses many cycles of PCR to amplify a desired file's corresponding DNA strands (referred to as random access[8,9,11,15,16]). However, random access is theoretically predicted to exhibit decreasing sequencing efficiencies with increasing database size as eventually PCR will not be able to overwhelm large quantities of nontarget database strands. To experimentally measure this transition point, we generated a library of five files, each with unique PCR primer sequences (Figure 2a, Supplementary Figure 2a), and mixed it with increasing quantities of background database strands. As it is currently cost prohibitive to order large databases of completely unique strands of DNA, large DNA databases can be mimicked in mass proportions by mixing copies of an individual file (i.e., 1.94 "nonunique" GB of File 3 strands = 1.14×10^9 total strands) with many more background database strands (i.e., 6.22 GB to 19.4 TB of a single nonspecific DNA strand, 3.66×10^9 to 1.14×10^{13} total strands, respectively). After 30 cycles of random-access PCR to amplify File 3 from this series of databases, the relative abundance of File 3 strands to background DNA was compared by quantitative PCR. As predicted, the percentage of the sample that was File 3 monotonically decreased as a function of increasing background DNA (Figure 2b). File 3 fell below 50% of the total sample once the database size reached 31.1 GB and higher. Thus, in high-capacity systems, random access becomes ineffective for specific file retrieval.

To address this database capacity limitation, we sought to physically separate newly created copies of specific files from the database while preserving the original library, allowing for the nondestructive and efficient sequencing and analysis of only desired data. Inspired by prior examples of biotin-mediated separations of DNA,[18,19] we modified this approach to create moiety-labeled copies of target file strands while leaving original unmodified file strands in the database. We did this by using moiety-modified primers in one cycle of PCR to create chemically labeled copies of a desired file's DNA strands (Figure 2c). These labeled copies of individual files were then separated from the database of five files using magnetic beads and fully recovered, as confirmed by next generation sequencing (NGS) (Figure 2d, e, Supplementary Figure 2b−d). We also expanded this approach to three other distinct modification systems and showed they were all capable of efficient and complete file access (biotin−streptavidin, fluorescein−antibody, digoxigenin−antibody, polyA−polyT oligomers). NGS results indicated sequencing efficiencies above 86%, representing a reduction in wasted sequencing throughput. Of note, to access files in this manner, we found that only a single emulsion PCR cycle was needed to chemically label files prior to their separation from the database. Importantly, we observed no destruction of the original database in the remaining solution following separation (Figure 2d, e, Supplementary Figure 2d). Furthermore, we determined that the same or a different file could be repeatedly accessed from this previously "used" database solution (Figure 2d). Taken together, this approach to physically separate files is nondestructive and represents a reusable DNA-based storage system.

To directly compare the performance of DENSE storage with random access in high-capacity systems, we compared the relative enrichments of File 3 from a 5.53-TB database (Figure 2f, g). In this experiment, to better mimic a true high-capacity and high-diversity database, File 1 was mutagenized by two rounds of error prone PCR[20] to an estimated 5.53 TB of unique data. Whereas random access was not able to significantly enrich File 3 strands from this high-capacity database, all four DENSE separation methods enriched File 3 to above 99% of the total sample after 30 cycles of emulsion PCR using the corresponding chemically modified primers.

High-capacity systems require many unique addresses to store and access information, yet there are roughly 28 000

DOI: 10.1021/acssynbio.9b00100
ACS Synth. Biol. 2019, 8, 1241−1248

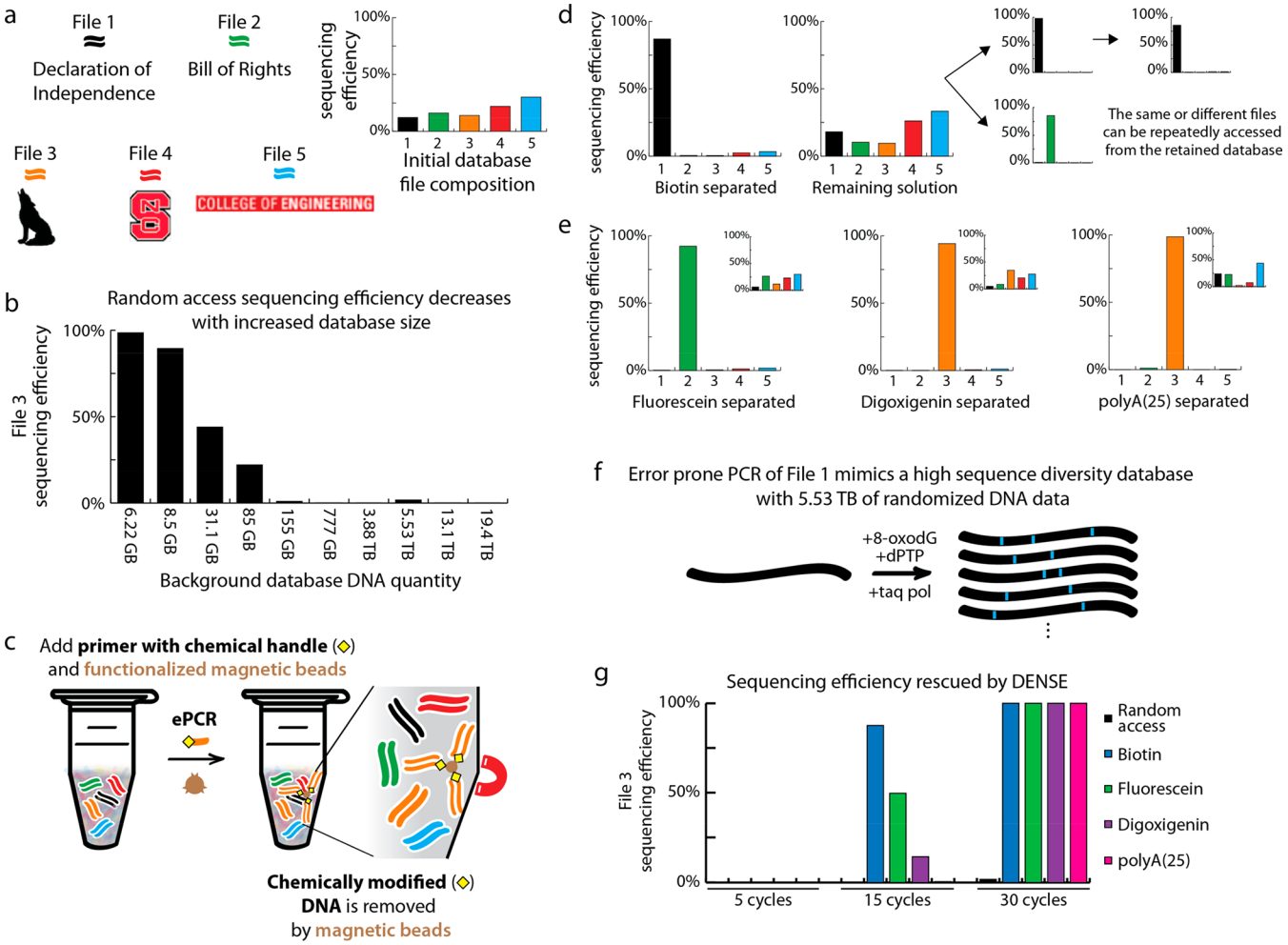

Figure 2. Physical file separations in DENSE storage rescue the decreased sequencing efficiency experienced by high-capacity databases. (a) A library of five files was ordered and analyzed using NGS to confirm an even file distribution. (b) File 3 strands were enriched over increasingly higher capacity backgrounds of nonspecific DNA strands using 30 cycles of random-access PCR. Random access failed to enrich File 3 to above 50% of the total sample once the background capacity reached 31.1 GB, as measured by quantitative PCR. (c) DENSE physically extracts a file (orange) from the database so only its strands are sequenced. A primer functionalized with a chemical handle (yellow diamond) is used to execute one emulsion PCR cycle to create chemically labeled copies of the desired file's strands. Functionalized magnetic beads (brown) that bind to the chemical handle are added to the sample. The desired file is bound to the bead, and the unbound solution containing the original database is removed and saved for future reuse. The bound file is then eluted from the bead. (d) After biotin–streptavidin file extractions, the remaining solution still contained all files, while the target files were enriched and physically separated, as measured by NGS. By mapping sequencing reads to the original file sequences, all targeted data were confirmed recovered. The target file was retained in the supernatant containing the database and was able to be copied and extracted again. File 1 was extracted three sequential times, and File 2 was extracted from the solution remaining after an initial extraction of File 1. (e) File extractions using fluorescein, digoxigenin, and polyA(25) as chemical handles also successfully separated target files from the database. (f) A large-scale background mimicking diverse data was created using error prone PCR[20] to mutagenize and amplify File 1. (g) Random access was compared directly to chemical handle extractions. File 3 strands, with a starting fraction of 0.025% of the total number of strands, were enriched over a high-capacity background equivalent to 5.53 TB of undesired, nonspecific strands using either random access (black) or PCR followed by chemical handle primer extractions (blue, green, purple, or pink). After 5, 15, and 30 cycles of PCR (random access), enrichment of File 3 was 0.0, 0.0, and 1.69% of the total sample, respectively. After biotin-modified PCR followed by extraction, the enrichment of File 3 was 0.2, 87.5, and 100% of the total sample, respectively. After fluorescein-modified PCR followed by extraction, the enrichment of File 3 was 0.1, 49.6, and 100% of the total sample, respectively. After digoxigenin-modified PCR followed by extraction, the enrichment of File 3 was 0.2, 14.2, and 100% of the total sample, respectively. After poly(A)-25-modified PCR followed by extraction, the enrichment of File 3 was 0.09, 0.47, and 100% of the total sample, respectively.

usable primer addresses that will not cross interact.[15] Thus, in a storage system comprised of 3 GB file sizes, 28 000 primers limit total system capacity to ~84 TB (Figure 1, "Single primer encoding"), given our strand organization and encoding strategy. To address this database capacity limitation, we were inspired by nested PCR architectures that were previously posed as a way to expand the number of possible addresses.[14] We integrated this strategy into DENSE by using a hierarchical encoding scheme where primer sequences are nested and used in sequential combination (Figure 3a). Theoretically, this architecture can more than exponentially increase the number of unique addresses for files without increasing the total number of unique primers needed: nesting two primers would increase theoretical system capacity by five orders of magnitude to enable exascale capacities (Figure 1, "Two primer hierarchy encoding"), while nesting more than two

DOI: 10.1021/acssynbio.9b00100
ACS Synth. Biol. 2019, 8, 1241–1248

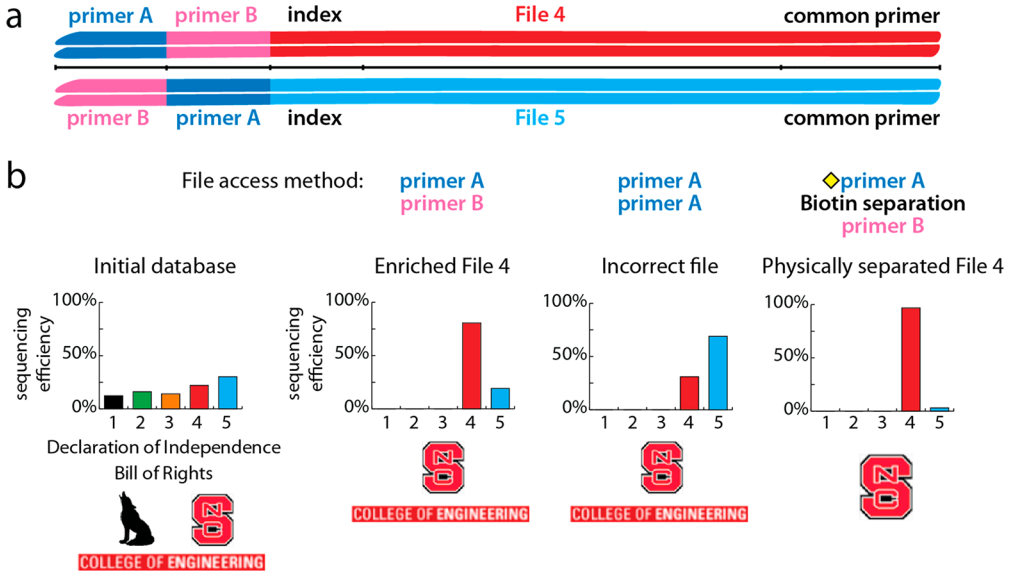

Figure 3. Combining a nested, hierarchical address strategy with physical separations results in purified enrichment of the desired file. (a) Strand architectures of Files 4 and 5 exhibit nested primer addresses. Binding sites for primers A and B are shared by both files but in opposite orders. Both files share a common antisense primer. (b) Experimental demonstration that PCR using primer A followed by primer B enriches for File 4. PCR amplification using two rounds of the same primer enriches for the incorrect file. In conjunction with physical extractions, File 4 is specifically accessed using hierarchical PCRs. The extraction after the first PCR amplification increases File 4 enrichment from 81 to 97% over no extraction, as measured by qPCR.

primers would result in exponentially larger numbers of total addresses (i.e., 28 000 unique primers$^{N \text{ number of nests}}$). Using this hierarchical PCR architecture with nested primers used in sequential combination (but with no physical extractions), both File 4 and File 5 were separately and selectively accessed using opposite temporal amplification sequences, albeit there were substantial amounts of contaminating off-target strands (Figure 3b, Supplementary Figure 3). This contamination arises because the original strands of both File 4 and File 5 are still present in the second PCR step, and both files would therefore be amplified in both PCR steps. This problem would be further exacerbated in higher capacity systems because of the high background and larger file sizes. Therefore, we combined this hierarchical strategy with biotin separations after each PCR step to remove the background strands (including the undesired contaminating file) and saw a reduction of these contaminating off-target strands. Specifically, the desired file in each case comprised either 96.9 or 86.8% of the sample, as measured by quantitative PCR, showing the specificity of nested addresses when used in the correct hierarchical temporal sequence and in conjunction with file separation (Figure 3b, Supplementary Figure 3).

DENSE is practical in that it reduces the number of PCR cycles needed compared to random-access methods: only one cycle was necessary to access data from the five-file database. This reduces not only the amount of dNTPs and other reagents needed but also the chances of mutational errors and alterations in strand distributions that may arise from PCR (Supplementary Figures 4−6). Consequently, in conjunction with DENSE, encoding algorithms may not need to sacrifice as much information density toward error correction. We do note that when the capacities of databases increase, more PCR cycles are required to access target files using DENSE (Figure 2g). At higher capacities, DENSE outperforms PCR alone (random access was not able to access target files at all), but this requirement for increased PCR cycles suggests additional biochemical engineering should be pursued to improve the specificities and affinities of the many complex molecular interactions that can occur during file separation.

Although initially designed to address barriers to scaling to the extreme capacities anticipated in the future (~PB and higher), DENSE storage is already useful and needed for smaller and imminently achievable capacities. For example, while the largest system created to date is 200 MB,[15] GB or TB amounts of DNA are routinely achieved by mainstream DNA synthesis companies in their aggregate purchase orders. Even for such modest systems, if common file sizes of ~25 MB are desired, there will be challenges in providing enough unique addresses without harnessing nested address architectures (Supplementary Figure 1, "25 MB files"). These nested architectures will also need to be integrated with physical file separations to avoid obtaining undesired contaminating strands, as each sequential PCR would otherwise have all database files available as templates, defeating the purpose of a nested architecture. Furthermore, without physical file separations, reading data from GB to TB level systems will be wasteful and perhaps infeasible even using state-of-the-art sequencing capabilities. For instance, Illumina's NovaSeq6000 can read only 20−30 GB of data when conservatively accounting for 10 redundant copies per strand (i.e., read depth of 10) (Figure 1, Supplementary Figure 1). Critically, this work demonstrates the enrichment and physical separation of 9.15 unique kBs of targeted DNA strands from 5.53 unique TBs of undesired database strands (Figure 2g). When considering the file's raw capacity instead of unique data, DENSE was able to enrich 1.94 GB of nonunique DNA strands from 5.53 TB of background strands. In other words, target strands starting at only 0.025% of the original database were enriched to over 99% purity in the separated sample. Therefore, as systems continue to scale, DENSE could be used to store and access individual files containing at least GBs of data. Thus, this file access approach can be combined with a

DOI: 10.1021/acssynbio.9b00100
ACS Synth. Biol. 2019, 8, 1241−1248

hierarchical, nested-address system to increase the theoretical total capacity of DNA storage systems by over five orders of magnitude (see Figure 1, Supplementary Figure 1, and eqs 1 and 2 in the Methods section for calculations).

While there are many challenges, and likely many still unanticipated, there are recent promising breakthroughs in all necessary aspects of DNA storage: advances continue to be made in DNA synthesis and sequencing, encoding and error correction, and physical file access and system architecture. This work provides a conceptual and quantitative framework to think about DNA storage systems and their challenges, proposes practical strategies to address key barriers to scaling system capacities, and suggests that DNA-based data storage systems with reasonable modern capacities and file access capabilities are not only immediately achievable but also scalable to extreme capacities in the future.

METHODS

Data Representation, Encoding, and Decoding. We adopted an approach for representing and encoding data similar to that reported in recent work.[6,9,15] We partitioned a digital file into blocks of data that fit in DNA strands that are 200 bp long. Each strand consists of multiple fields. A primer binding site occupies each end and enables DNA polymerase chain reactions. Between the primers, we placed three fields that represent the index of the strand within the file, the data payload, and a checksum to detect errors within the strand. We used a fixed length index that is 16 bp-long and a fixed length checksum that is 8 bp-long. This leaves the remaining 136 bp-long sequence to represent the data payload of each strand. We designed 8 bp-long codewords to represent one byte of data. The codewords have no repetition of bases both individually and when appended, and they are GC balanced. Each byte of file is converted one byte at a time into a corresponding codeword and appended together to form the payload of a strand. The checksum is a single-byte XOR-accumulation of all the data in the payload that is encoded and appended to the end of the data payload. The checksum allows each strand to self-check its own data. The only notable difference for hierarchical encoding is that it requires an additional primer binding site in each strand, thereby reducing the size of the data payload.

We also adopted a redundant XOR-style encoding proposed by Bornholt et al.[9] to enhance the reliability of our system. In our design, indices with even values hold data, and odd indices store the XOR-ed content of their adjacent strands. This redundancy enables recovery of data even if some strands are lost or discarded due to an invalid checksum. The decoder algorithm for our encoding is similar to that used in previous work[9] with the modification that we can disregard any read with an invalid checksum. It is important to note that for clarity of analysis and ease of comparison across systems, the file and database sizes estimated in the figures do not take into account the overhead required to implement XOR or other encodings that may be used. Thus, we present best case scenarios, whereas true capacity challenges and limitations are likely even more severe than described in this work.

Primer Design. Primers used in this work were designed to achieve multiple goals. First, they must facilitate effective PCRs. The primers were designed such that GC content is between 40 and 60%, and their melting temperature is between 50 and 60 °C. We required that the last base is G, but the GC content in the last 5 bases could not exceed 60%. Second, primers were designed to reduce the likelihood of nonspecific binding with other primer binding sites. We required a Hamming distance of >10 between all primers to minimize the likelihood of such binding. We also performed NUPACK simulations of homodimer, hairpin, and heterodimer bindings.[21] We required a Gibbs free energy greater than −10 kcal/mol at 50 °C on all likely complexes to select the primer. Note, we compared each candidate primer to all other primers to ensure no heterodimer bindings are likely, and we included the Illumina NEXTERA primers in this process. Third, to reduce the likelihood of nonspecific binding between a primer and the data payload, we required that primers must contain a repeating nt every 5 bases. This guaranteed that primers would differ from all length 20 subsequences of the data payload.

We used a computer program written in Python to automate the generation of candidate primer sequences and screened them against the requirements stated above. The python program invoked the relevant analysis in NUPACK as needed.

Emulsion PCR. The emulsion PCR (ePCR) protocol from Schutze et al.[22] was modified slightly and used for all PCR steps. Emulsions were created by mixing 150 μL of emulsion oils (73% v/v Tegosoft DEC (Evonik, 99068594), 20% v/v mineral oils (Sigma-Aldrich, 330779), and 7% ABIL WE (Evonik, 99068358)) with 25 μL aqueous PCR samples. Samples were then vortexed for 5 min until a persistent emulsion was formed. Samples were aliquoted into four PCR tubes, and a standard Q5 polymerase PCR protocol was used. Twenty cycles were sufficient to reach the maximum yield of DNA product. After amplification, aliquots were pooled in an Eppendorf tube and emulsions were broken with the addition of 1 mL of isobutanol followed by a 5 s vortex. Five volumes of (125 μL for 25 μL PCR reaction volume) binding buffer (Biobasic Canada Inc. BS664) was added to samples, gently mixed, and centrifuged at 2400*g* for 30 s. The organic phase was removed and discarded while the remaining aqueous phase was purified using AMPure XP beads (Beckman Coulter, A63881). DNA was eluted in 50 μL of water.

Biotin−Streptavidin File Extractions. File-specific sense ("coding") primers were ordered with a biotin modification on the 5′ end. PCR amplified samples were purified (AMPure XP beads) and added to prewashed streptavidin magnetic beads (NEB #S1420S) (wash and bind buffer: 20 mM Tris-HCl pH 7.4, 2 M NaCl, 2 mM EDTA pH 8) and incubated at room temperature on a rotisserie for 30 min. The database files were retained by collecting the supernatant. The beads were then washed once with 100 μL of the binding buffer and once with 100 μL of a low-salt wash buffer (20 mM Tris-HCl pH 7.4, 150 mM NaCl, 2 mM EDTA pH 8). Amplified DNA was subsequently eluted (elution buffer: 95% formamide (Sigma, F9037) in water). DNA sizes and concentrations of the purified (AMPure XP beads) supernatants and elutions were measured on a Fragment Analyzer (Advanced Analytical, DNF-474) before the addition of Illumina sequencing adapters. Representative DNA gel images of biotin separations are shown in Supplementary Figure 2b.

Fluorescein and Digoxigenin File Extractions. File-specific sense ("coding") primers were ordered with either fluorescein or digoxigenin on the 5′ end (Eurofins Genomics). Antibodies (anti-fluorescein: Novus Biologicals, NB600-493, Lot 19458; anti-Digoxigenin (21H8): Novus Biologicals, NBP2-31191, 17E16) were bound to magnetic protein A or G beads (BioRad Cat. # 161-4013 and 161-4023) through a 30

DOI: 10.1021/acssynbio.9b00100
ACS Synth. Biol. 2019, 8, 1241−1248

min room temperature incubation (bind and wash buffer: 20 mM Tris-HCl pH 8, 300 mM NaCl, 2 mM EDTA). PCR amplified samples were purified (AMPure XP beads) and added to the antibody-linked beads and incubated at room temperature on a rotisserie for 2 h. The database files were retained by collecting the supernatant. The beads were washed once with 100 μL of the binding buffer and once with 100 μL of a low salt wash buffer (20 mM Tris-HCl pH 7.4, 150 mM NaCl, 2 mM EDTA pH 8). DNA sizes and concentrations of the purified (AMPure XP beads) supernatants and elutions were measured on a Fragment Analyzer (Advanced Analytical, DNF-474) before the addition of Illumina sequencing adapters. Representative DNA gel images of a fluorescein separation are shown in Supplementary Figure 2c.

Oligo-d(T) Magnetic Bead Separation. File-specific sense ("coding") primers were ordered with a poly(A)-25 tail on the 5′ end (Eurofins Genomics). Oligo-d$(T)_{25}$ beads (NEB #S1419S) were washed twice with 100 μL wash and bind buffer (20 mM Tris-HCl pH 7.4, 2 M NaCl, 2 mM EDTA pH 8). PCR amplified samples were purified (AMPure XP beads) and added to the desired amount of bead based on the amount of DNA present and theoretical binding capacity. The mixture was heated in a thermal mixer at 90 °C and 500 rpm for 2 min, allowed to cool to room temperature, and the database files were retained by removing the supernatant. The beads were washed twice with 100 μL of a low salt wash buffer (20 mM Tris-HCl pH 7.4, 150 mM NaCl, 2 mM EDTA pH 8). Beads were then resuspended in 1× TE buffer and heated in the thermal mixer at 50 °C and 500 rpm for 2 min. The desired file was extracted while the mixture was still hot by removing the eluted sample from the beads. DNA sizes and concentrations of the purified (AMPure XP beads) supernatants and elutions were measured on a Fragment Analyzer (Advanced Analytical, DNF-474) before the addition of Illumina sequencing adapters.

Calculation of Data Quantity from Total Number of DNA Strands. In Figures 1, 2, and Supplementary Figures 1 and 2, we refer to file and database sizes (MB, GB, etc.). For clarity and ease of comparison, all values were calculated based on the total number of DNA strands. Each strand is comprised of 200 nts, 20 of which are used for each primer sequence, 16 for the index, and 8 for the checksum. Eight nts comprise each 1-byte codeword. Thus, each strand addressed with a single primer pair contains 17 bytes of data. Specifically, in Figure 2, we assumed a 10-copy physical redundancy per unique strand to provide a conservative estimate for a realistic system where multiple copies of each strand would likely be needed to avoid strand losses and inhomogeneous strand distributions. Thus, in Figure 2 total file and database sizes are divided by 10.

Calculation of System Capacity. In Figure 1 and Supplementary Figure 1, we calculate the system capacity by following eq 1 and eq 2.

$$\text{system capacity}(B) = PUD \tag{1}$$

$$\text{strand density}(\text{B/strand}) = \frac{\text{strand length} - \text{strand overhead}}{\text{encoding density}} \tag{2}$$

Where P is the number of primers available to the system, U is the number of unique strands that can be supported for each file, and D is strand density in units B/strand. The density, D, in B/strand can be calculated by dividing the number of bases available for data encoding by the encoding density in units of B/base. For Figure 1 and Supplementary Figure 1, we start with a strand length of 200 and subtract off the overhead associated with both flanking primers, which will be a total of 40 bases in the case of a single primer system and 60 bases in the case of a hierarchical primer system. The leftover bases can then be either allocated to the index region of the strand or to the payload region. With the number of bases selected for the index region, the number of unique strands supported for each file, U, can then be determined by applying the encoding method utilized by the system for the index. In our examples, we conservatively choose a base-3 encoding; thus, U will be equal to 3^N, where N is the number of bases allocated to the index region. With the remaining bases, strand density can be calculated by dividing the number of remaining bases by the encoding density in units of B/base, where in our examples, we conservatively choose an encoding density of 0.125 B/base (8 bases for each byte).

Error Prone PCR. Template DNA was amplified using 0.5 μL of Taq DNA polymerase (5 units/μL, Invitrogen, 100021276) in a 50 μL reaction containing 1× Taq polymerase Rxn Buffer (Invitrogen, Y02028), 2 mM MgCl2 (Invitrogen, Y02016), the sense and antisense primers at 1E13 strands each, and dATP (NEB, N0440S), dCTP (NEB, N0441S), dGTP (NEB, N0442S), dTTP (NEB, N0443S), dPTP (TriLink, N-2037), and 8-oxo-dGT (TriLink, N-2034), each at 400 mM. PCR conditions were 95 °C for 30 s, 50 °C for 30 s, and 72 °C for 30 s for 35 cycles with a final 72 °C extension step for 30 s.

qPCR. qPCR was performed using SsoAdvanced Universal SYBR Green Supermix (BioRad). qPCRs were performed in 5 μL format using SYBR Green (95 °C for 2 min and then 50 cycles of: 95 °C for 10 s, 50 °C for 20 s, and 60 °C for 20 s). qPCR results were compared to next generation sequencing results for samples that were analyzed using both methods. File compositions measured using both methods showed strong agreement (Supplementary Table 1).

Illumina Library Preparation. Illumina TruSeq Nano DNA Library Preps (Illumina, 20015965) were performed according to manufacturer instructions beginning from the "Repair Ends and Select Library Size" step, as DNA fragmentation was unnecessary. The quality and band sizes of libraries were assessed using the High Sensitivity NGS Fragment Analysis Kit (Advanced Analytical, DNF-474) on the 12 capillary Fragment Analyzer (Advanced Analytical) at multiple steps during each protocol, typically after size selection and PCR amplification. Unless otherwise stated, libraries were normalized to balance estimated sequencing depth across similar samples (e.g., all elutions had estimated sequencing depth of ∼100 reads) using the molar concentrations measured on the Fragment Analyzer. The pooled sample had a concentration of 8 nM and was sequenced using the MiSeq v2 chemistry 150 PE kit that was operated as a 300 SR run. PhiX DNA was added at 20% of total DNA to increase sequence diversity.

Error Analysis. Before proceeding with an error analysis of sequenced strands, the error-free reference strand for each sequenced strand needed to be determined. To find the error-free reference strands, a mapping operation was performed to match each sequenced strand with its original database strand. Due to the large number of sequenced strands in samples (up to 571k reads), the mapping operation was carried out in two steps: the first step partitioned the large read space using the

DOI: 10.1021/acssynbio.9b00100
ACS Synth. Biol. 2019, 8, 1241−1248

primer sequences of the different files, and the second step further analyzed each partition to match each strand in a partition with its corresponding database strand.

The first step of mapping divided the initial sequencing read space into partitions, one for each file in the database, with the exception of Files 4 and 5 (hierarchical encodings) where each of these files had two partitions. These two partitions were used to separate nested address strands that were truncated from the first PCR step and reads where the nested address strands were not truncated. Other partitions were also created for special strands like the background strands used to simulate high-capacity data storage and for unknown strands that could not be categorized into a file's partition. A strand from sequencing was placed into a partition by looking for a subsequence that matched a file's sense primer or the reverse complement of the antisense primer. The reverse complement of the antisense primer was used because all NGS sequencing reads are in the 5′ to 3′ direction. A subsequence was deemed acceptable if it matched a sense primer or antisense primer's reverse complement within a Levenshtein distance of 4. A Levenshtein distance of 4 was chosen as the cutoff point to ensure that the matched subsequence was not data within a DNA strand, but one of the primers of interest. When a primer of interest is found in a sequenced strand, the sequenced strand is placed in the primer's respective partition.

After categorizing each strand in a sample's sequence pool, each partition was analyzed further to determine the original database strand for each sequenced strand in the partition. To find out the correct original strand, each original strand from a file was compared to each sequenced strand placed in the file's partition by calculating the Levenshtein distance between the sequenced strand and the original strand. If the distance was less than or equal to 12, the original strand was considered as a candidate for a match. Because some of the original strands in the database have small edit distances between them, file strands that are close to the candidate were also checked against the sequenced strand to make sure the correct original strand was chosen. Once a candidate was concluded to correspond to a specific original strand, the location of the matching strand in the file along with the sequenced strand's location in the read space was recorded. A distance of 12 was chosen as the threshold to reduce the amount of checking that was required once a candidate was found, while ensuring that error rates would not be artificially low due to choosing candidates that were within a small number of edit operations.

With a completed mapping of sequenced strands to their corresponding database strands, analyses such as error rates per base, strand error rates, and read distributions were performed. To calculate the error rate for a nt position, eq 3 was used, where L is the number of unique edit operations considered (insertions, deletions, substitutions), M is the number of unique strands in the database, s_j is the jth strand in the database, N_j is the number of sequenced strands that map to strand s_j, s_k is the kth strand that maps to database strand s_j, T is the total number of strands from the sample that has been mapped to some database strand, and $\mathrm{EO}_l(s_j, s_k)_i$ is the number of edit operations of type l at the ith nt position to transform s_j to s_k. This equation calculates the total error rate for base position i by summing all of the edit operations of each type at the ith position needed to transform each original database strand to the sequenced strands that map to it and then dividing by the total number of mapped strands in the sample.

$$\text{total error rate}_i = \frac{\sum_{l=1}^{L}\sum_{j=1}^{M}\sum_{k=1}^{N_j}\mathrm{EO}_l(s_j, s_k)_i}{T} \quad (3)$$

Similarly, the error rate for each strand in the original database was calculated using eq 4, where L is the number of unique edit operations, s_j is a strand from the original database, N_j is the number of sequenced strands that map to strand s_j, s_k is the kth strand that maps to s_j, T_{sj} is the total number of mappings in the sample for s_j, and $\mathrm{EO}_l(s_j, s_k)$ is the number of edit operations of type l to transform s_j to s_k.

$$\text{total error rate}_{s_j} = \frac{\sum_{l=1}^{L}\sum_{k=1}^{N_j}\mathrm{EO}_l(s_j, s_k)}{T_{s_j}} \quad (4)$$

■ ASSOCIATED CONTENT

Supporting Information

The Supporting Information is available free of charge on the ACS Publications website at DOI: 10.1021/acssynbio.9b00100.

Supplementary Figures 1−6; Supplementary Table 1, including quantitative analyses; library description, preliminary data, and complete analysis of file separations; PCR amplifications; strand distributions; error rate heatmaps; and comparison of next generation sequencing and qPCR measurements of file ratios within samples (PDF)

■ AUTHOR INFORMATION

Corresponding Authors

*E-mail: jtuck@ncsu.edu.
*E-mail: ajkeung@ncsu.edu.

ORCID

Kyle J. Tomek: 0000-0002-2417-836X
Albert J. Keung: 0000-0001-8958-1232

Author Contributions

⊥These authors contributed equally to this work. K.J.T., J.T., and A.J.K. conceived the study. K.J.T., E.W.I., and A.J.K. developed the wet experimental system. K.V., A.S., and J.T. developed the software and simulations. K.J.T., E.W.I., A.G.H., and A.J.K. planned and performed the wetlab experiments with guidance from all. K.V., A.S., and J.T. planned and performed simulations and next generation sequencing analysis with guidance from all. K.J.T., A.J.K., K.V., and J.T. wrote the paper with input from all.

Notes

The authors declare no competing financial interest.

■ ACKNOWLEDGMENTS

We acknowledge Kevin N. Lin for helpful discussions. This work was supported by the National Science Foundation (Grant CNS-1650148), a North Carolina State University Research and Innovation Seed Funding Award (Grant 2018-2509), and the North Carolina Biotechnology Center Flash Grant to A.J.K. and J.T. K.J.T. was supported by a Department of Education Graduate Assistance in Areas of Need Fellowship. E.W.I. and A.H. were supported by funds from the North Carolina State University Research Experience for Undergraduates, Provost's Professional Experience Programs, and NCSU startup funds.

DOI: 10.1021/acssynbio.9b00100
ACS Synth. Biol. 2019, 8, 1241−1248

REFERENCES

(1) Cox, J. P. L. (2001) Long-Term Data Storage in DNA. *Trends Biotechnol. 19*, 247−250.

(2) Orlando, L., Ginolhac, A., Zhang, G., Froese, D., Albrechtsen, A., Stiller, M., Schubert, M., Cappellini, E., Petersen, B., Moltke, I., et al. (2013) Recalibrating Equus Evolution Using the Genome Sequence of an Early Middle Pleistocene Horse. *Nature 499*, 74−78.

(3) Grass, R. N., Heckel, R., Puddu, M., Paunescu, D., and Stark, W. J. (2015) Robust Chemical Preservation of Digital Information on DNA in Silica with Error-Correcting Codes. *Angew. Chem., Int. Ed. 54*, 2552−2555.

(4) Zhirnov, V., Zadegan, R. M., Sandhu, G. S., Church, G. M., and Hughes, W. L. (2016) Nucleic Acid Memory. *Nat. Mater. 15*, 366−370.

(5) Church, G. M., Gao, Y., and Kosuri, S. (2012) Next-Generation Digital Information Storage in DNA. *Science 337*, 1628.

(6) Goldman, N., Bertone, P., Chen, S., Dessimoz, C., LeProust, E. M., Sipos, B., and Birney, E. (2013) Towards Practical, High-Capacity, Low-Maintenance Information Storage in Synthesized DNA. *Nature 494*, 77−80.

(7) Shah, S., Limbachiya, D., and Gupta, M. K. (2014) DNACloud: A Potential Tool for Storing Big Data on DNA. *Cornell University*, arXiv: 1310.6992.

(8) Yazdi, S. M. H. T., Yuan, Y., Ma, J., Zhao, H., and Milenkovic, O. (2015) A Rewritable, Random-Access DNA-Based Storage System. *Sci. Rep. 5*, 14138.

(9) Bornholt, J., Lopez, R., Carmean, D. M., Ceze, L., Seelig, G., and Strauss, K. (2016) A DNA-Based Archival Storage System. *ASPLOS '16*, 637−649.

(10) Blawat, M., Gaedke, K., Huetter, I., Chen, X.-M., Turczyk, B., Inverso, S., Pruitt, B., and Church, G. (2016) Forward Error Correction for DNA Data Storage. *Procedia Comput. Sci. 80*, 1011−1022.

(11) Yazdi, S. M. H. T., Gabrys, R., and Milenkovic, O. (2017) Portable and Error-Free DNA-Based Data Storage. *Sci. Rep. 7*, 5011.

(12) Erlich, Y., and Zielinski, D. (2017) DNA Fountain Enables a Robust and Efficient Storage Architecture. *Science 355*, 950−954.

(13) Agrawal, A., Limbachiya, D., M, R., Saiyed, T., and Gupta, M. K. (2019) BacSoft: A Tool to Archive Data on Bacteria. *Cornell University*, arXiv: 1903.01902.

(14) Kashiwamura, S., Yamamoto, M., Kameda, A., Shiba, T., and Ohuchi, A. (2003) Hierarchical DNA Memory Based on Nested PCR. *DNA8, LNCS 2568*, 112−123.

(15) Organick, L., Ang, S. D., Chen, Y.-J., Lopez, R., Yekhanin, S., Makarychev, K., Racz, M. Z., Kamath, G., Gopalan, P., Nguyen, B., et al. (2018) Random Access in Large-Scale DNA Data Storage. *Nat. Biotechnol. 36*, 242−249.

(16) Organick, L., Chen, Y., Ang, S. D., Lopez, R., Strauss, K., and Ceze, L. (2019) Experimental Assessment of PCR Specificity and Copy Number for Reliable Data Retrieval in DNA Storage. *bioRxiv*, DOI: 10.1101/565150.

(17) Zakeri, B., Carr, P. A., and Lu, T. K. (2016) Multiplexed Sequence Encoding: A Framework for DNA Communication. *PLoS One 11*, e0152774.

(18) Adleman, L. M. (1994) Molecular Computation of Solutions to Combinatorial Problems. *Science 266*, 1021−1024.

(19) Stewart, K., Chen, Y.-J., Ward, D., Liu, X., Seelig, G., Strauss, K., and Ceze, L. (2018) A Content-Addressable DNA Database with Learned Sequence Encodings. *DNA Comput. Mol. Program. 11145*, 55−70.

(20) Zaccolo, M., and Gherardi, E. (1999) The Effect of High-Frequency Random Mutagenesis on in Vitro Protein Evolution : A Study on TEM-1 b -Lactamase. *J. Mol. Biol. 285*, 775−783.

(21) Zadeh, J. N., Steenberg, C. D., Bois, J. S., Wolfe, B. R., Pierce, M. B., Khan, A. R., Dirks, R. M., and Pierce, N. A. (2011) Software News and Updates NUPACK: Analysis and Design of Nucleic Acid Systems. *J. Comput. Chem. 32*, 170−173.

(22) Schütze, T., Rubelt, F., Repkow, J., Greiner, N., Erdmann, V. A., Lehrach, H., Konthur, Z., and Glökler, J. (2011) A Streamlined Protocol for Emulsion Polymerase Chain Reaction and Subsequent Purification. *Anal. Biochem. 410*, 155−157.

DOI: 10.1021/acssynbio.9b00100
ACS Synth. Biol. 2019, 8, 1241−1248